Structural Studies of the Water Tetramer

JHON F. PÉREZ, C. Z. HADAD, ALBEIRO RESTREPO

Grupo de Química-Física Teórica, Instituto de Química, Universidad de Antioquia, AA 1226 Medellín, Colombia

ABSTRACT: In this article, we report the geometries and properties of the structural isomers obtained from a random walk of the potential energy surface of the water tetramer. Eight structures were obtained after B3LYP/6-311++G** and MP2/6-311++G** optimization of 59 candidate structures generated from a stochastic search of the PM3 conformational space. The random search was carried out using a recently proposed modified Metropolis acceptance test in the simulated annealing procedure. Highly correlated CCSD(T)/6-311++G** energies on the MP2 geometries were calculated and used to determine relative stabilities and to estimate isomer concentrations. We obtained three different geometrical motifs: planar cyclic tetramers, planar cyclic trimers interacting with an extra off-plane water molecule, and a bicycle-like structure. Our CCSD(T) energies, in agreement with previous reports, predict the global minimum to be a planar cyclic tetramer with hydrogen atoms alternating above and under the plane.   © 2008 Wiley Periodicals, Inc. Int J Quantum Chem 108: 1653–1659, 2008

Key words: water clusters; hydrogen bond networks; stochastic optimization; modified metropolis test; ab initio calculations

1. Introduction

The effects of cooperative hydrogen bond systems have been for a long time a topic of intensive research in areas as diverse as Physics, Chemistry, and Biology. Countless manifestations of the hydrogen bonds, from the structures of liquid water, and DNA to interstellar chemistry are routinely published. In a recent study, for example [1],

it was reported that hydrogen bonds play a pivotal role in the molecular interactions which are responsible for the stabilization of (ethanol)$_2$–water clusters, an observation that can be extrapolated to the interactions of larger clusters, not unlike those responsible for the formation of the characteristic ethanol/water azeotrope that prevents complete separation of the mixtures by distillation. Despite its relevance, many important aspects of weakly hydrogen bonded systems remain unclear [2], probably due in part to the complexity of energy decomposition schemes for this kind of interactions [3],

which is difficult in achieving accurate theoretical treatments. Some authors for instance have suggested that cooperative polarization effects play a major part on this interaction [4], while others assign that role to cooperative charge transfer [5–7]. In any case, it seems firmly established that good accounts for electron correlation and extended basis sets are needed for proper descriptions. In the specific case of the water tetramer (W_4 here forth), Clementi and coworkers [8] as well as Wales and Walsh [9] have pointed out the high-sensitivity of the results obtained to the chosen level of theory.

Generation of cluster structures is a problematic subject. For small size clusters, systematic, intuition-guided construction of geometries until exhaustion of possibilities seems to be the methodology of choice; an alternative plan, employed by Miyake and Aida on the study of small water clusters [10], is to construct all the topologically distinct patterns for the system in question. However, said approaches quickly become impracticable because the number of stationary points in a given potential energy surface (PES) increases dramatically as a function of size [11, 12]. Under such circumstances, most reports concern themselves with locating and studying global minima for small to moderate size systems. The implicit drawbacks of such line of actions are: (1) to ignore local minima having significative probabilities of existence that could influence chemical and physical processes, and (2) it is not always possible to ensure that a *constructed* structure is indeed the global minimum. Since the geometries of clusters have considerable influence on measurable properties, a reliable method for exploring multidimensional PESs is in order.

Recently, we have proposed an application of a modified simulated annealing (SA) [13–15] optimization procedure with quantum evaluation of the energy (ASCEC after its Spanish acronym Annealing Simulado Con Energía Cuántica) as a tool for comprehensive generation of cluster candidate structures [16, 17]. The method incorporates the comparative advantages and disadvantages of stochastic optimization over analytical methods [11], namely, initial-guess independence, exhaustive exploration of the PES and the very desirable feature of avoiding being trapped in local minima by virtue of the ability to jump over energy barriers and to sample several energy wells on the same run; however, the method is still computationally intensive because of the repetitive evaluation of the energy function. Following the successful application of the ASCEC algorithm to the study of small neutral and charged Lithium clusters [16], in this article we report the first application of the method to the study of molecular clusters, choosing the W_4 system for the same reasons we first applied ASCEC to Lithium clusters: there is extensive literature on small water polymers to compare against our results as means of validating our method.

2. Computational Methods

We used the molecular cluster capabilities of the ASCEC program, which contains an adapted version of the SA optimization algorithm.

2.1. THE ANNEALING PROCEDURE

Brief description of the workings of ASCEC: The ASCEC program performs a random walk on the conformational space of the molecular cluster. The system is allowed to evolve inside a cubic box of user supplied length L, in agreement with the original algorithm proposed by Metropolis et al. [13] The ASCEC program calls the Gaussian 03 suite of programs [18] to calculate the quantum energy of every generated structure which is then the subject of an acceptance test. If the structural change lowers the energy ($\Delta E < 0$), then the move is accepted; in case $\Delta E > 0$, the new structure is accepted if $\Phi(\Delta E) < P(\Delta E)$, where $P(\Delta E) = \exp(-\Delta E/k_B T)$, is the temperature-dependent Boltzmann's probability distribution function and $\Phi(\Delta E) = \Delta E/E_j$, j being the structure under evaluation. We found the latter acceptance criterion to be more adequate in this line of problems than the usual procedure of comparing $P(\Delta E)$ to a randomly generated number in the [0, 1] range, where good structures can be randomly rejected. If neither test is satisfied, the move is not accepted and the structure that originated the change is randomly modified again. To avoid a large number of meaningless energy evaluations, a maximum number of structures can be generated at each temperature without satisfying either of the two acceptance criteria; that number (MaxCyc) is reduced every time it is reached. Relative positions and orientations between molecules belonging to a particular structure are simultaneously moved at random up to a maximum amount allowed. Only accepted structures are changed, effectively constructing a Markov chain of points in the conformational space. A flux diagram for the algorithm is sketched in Figure 1.
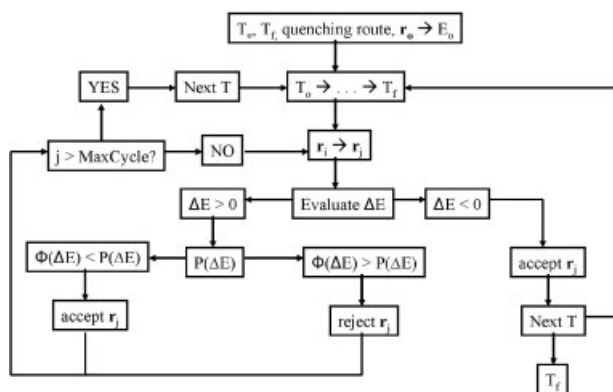
FIGURE 1. The SA procedure with a modified Metropolis test used to explore the PM3 conformational space of the water tetramer. The candidate structures produced by this procedure are further optimized by analytical methods at higher levels of theory.

A typical run of ASCEC requires the following user supplied information: (a) A quenching route: initial and final temperatures and a route connecting them; at present a choice between a linear (decreasing T by a constant amount) and a geometric (decreasing T by a constant percentage) routes is available. (b) The initial geometry in Cartesian coordinates. (c) A length for a cube in which the system evolves. (d) Maximum initial number of structures to be evaluated before going to the next temperature (MaxCyc). (e) Maximum allowed relative displacement and orientation changes for individual molecules within the current cluster structure. (f) A combination of Hamiltonian/basis set for energy calculations. The entire process of input generation for the Gaussian 03 calculations and the processing of its outputs are completely transparent to the user, so only ASCEC related files are to be manipulated. In this research, we used the PM3 semiempirical Hamiltonian (designed to treat hydrogen bonding)[19, 20] for energy calculations during ASCEC runs.

2.2. LOCATING AND TREATING STATIONARY POINTS

A successful ASCEC run generates a number of candidate structures which are then optimized by analytical methods. We used the hybrid B3LYP density functional [21–23] in combination with the 6-311++G** basis set to optimize and characterize the candidate structures afforded by ASCEC. Because several initial structures converged to the same equilibrium geometry, only a few stationary points were found by this procedure. For a better account of electron correlation, the more sophisticated MP2/6-311++G**[24, 25] methodology was used to further refine the B3LYP geometries. Analytical harmonic second derivatives calculations on both B3LYP and MP2 surfaces were used to characterize stationary points as true minima (no negative eigenvalues of the Hessian matrix) or saddle points. Highly correlated CCSD(T)/6-311++G**[26] energy calculations were carried out on the MP2 geometries in order to establish relative stability of the isomers. Isomer populations, x_i, within a given PES were estimated by [27]

$$x_i = \frac{g_i e^{-E_i/k_B T}}{\sum_i g_i e^{-E_i/k_B T}} \qquad (1)$$

where g_i is the degeneracy of isomer i and E_i the corresponding CCSD(T)//MP2 energy. All optimizations, frequency, and energy calculations were carried out using the Gaussian 03 [18] suite of programs.

3. Results and Discussion

3.1. ASCEC RESULTS

We used the Big Bang approach to construct the initial geometry for the ASCEC run, namely all water molecules were placed at the same position with the same orientation, allowing them to evolve under the Annealing conditions within a cube of 6 Å of length. The PM3 semiempirical Hamiltonian was used to calculate the energy of randomly generated cluster configurations. We used a geometrical quenching route with initial temperature of 500 K, a constant temperature decrease of 10% and 300 total temperatures. The Max-Cyc parameter was set to 1,000. The stochastic sampling generated 59 candidate structures, 45 of them after satisfying our modified Metropolis test ($\Delta E/E_j < \exp[-\Delta E/k_B T]$), the remaining 14 after a random move resulted in lowering the energy.

Figure 2 shows an energy profile for the ASCEC run of the W_4 cluster. Figure 3 is a plot of the number of accepted structures as a function of their temperature. A few features from Figures 2 and 3 are worth pointing out: the non-monotonical decrease in energy as the simulation proceeds clearly shows the ability of the algorithm to jump over energy barriers. Most of the accepted structures happen at early to intermedi-
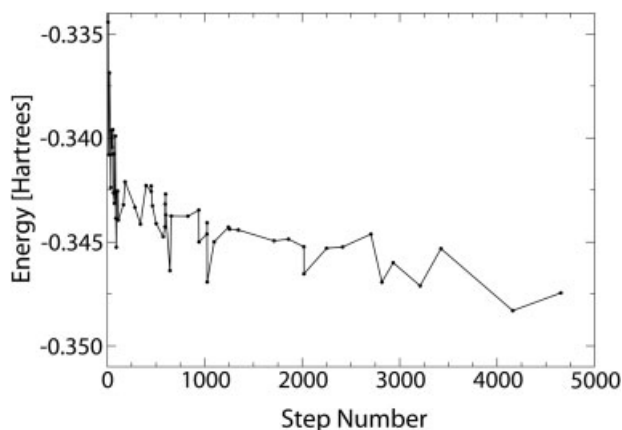
FIGURE 2. SA for the W_4 clusters. ASCEC conditions: Initial T = 500 K, constant decrease in T = 10%, number of temperatures: 300, cube length: 6 Å, MaxCyc = 1,000.

ate stages of the simulation, this can be attributed to the fact that as temperature lowers, satisfying either of the two acceptance criteria is increasingly harder. The last accepted configuration happens around 75 K, the simulation still runs down to lower temperatures. It can also be seen from Figures 2 and 3 that the lowest energy structure was not found at the lowest simulation temperature. All the above observations are consistent with what is expected from a robust and efficient implementation of the Annealing algorithm.

3.2. CLUSTER STRUCTURES

The B3LYP and MP2 equilibrium geometries were produced following the procedure described in the Methodology section. It is important to state that all geometry optimizations were carried with no imposition of symmetry constraints as the structures coming from ASCEC are randomly generated and belong to the C_1 point group; however, some of the located stationary points have higher symmetries (the final structures still belong to the C_1 point group as that is the symmetry of choice during optimizations, so geometrical parameters may differ near the last decimal places).

3.2.1. Geometries

We found eight equilibrium structures on both PESs (B3LYP, MP2) spread into the three different geometrical motifs shown in increasing order of energy in Figure 4. There are four planar cyclic

tetramers (structures I, II, III, and VIII), three of them (I, II, and III) exhibiting the same hydrogen bonded network, where each water molecule acts simultaneously as hydrogen bond donor and acceptor; in the remaining tetramer (VIII), two opposing molecules act as double donors while the other two act as double acceptors of the hydrogen bonds. We located three planar cyclic trimers interacting with an extra off-plane water molecule (structures V, VI, and VII in Fig. 4) and a bicycle-like conformation (structure IV). As a summary of our results compared against earlier works, Table I gives a partial account (not intended as a comprehensive review) of W_4 structures reported previously. Our literature search did not afford a match to any previous reports of structures III (a cyclic planar tetramer with three hydrogen atoms on the same side out of the plane) and VII (a cyclic planar trimer with one water molecule donating simultaneously to the cycle and to an off-plane water molecule and the two non hydrogen-bonded hydrogen atoms sticking below the plane).

3.2.2. Energies and Other Properties

Relative energies (ΔE), binding energies (BE), isomer populations ($\%x_i$), unscaled zero-point vibrational (ZPE), and Gibbs energies are shown in Table II. It can be observed that the lowest energy structure predicted by our methodology agrees with the global minimum reported in previous works (structure I). MP2/6-311++G** exhibits a similar PES to B3LYP/6-311++G** regarding structural and energetic parameters. Both methods
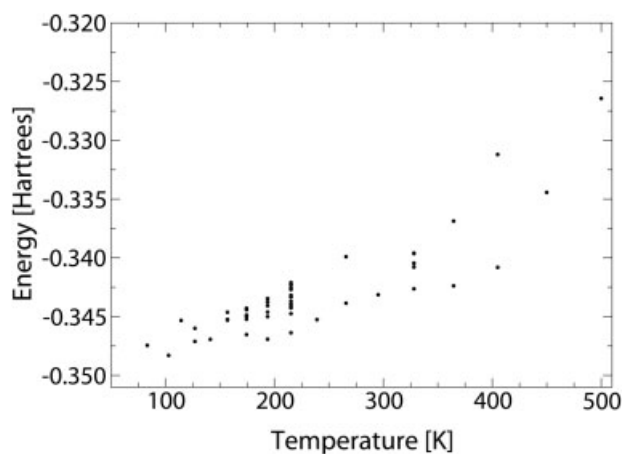

FIGURE 3. Candidate structures generated by AS-CEC for the W_4 clusters as a function of temperature.
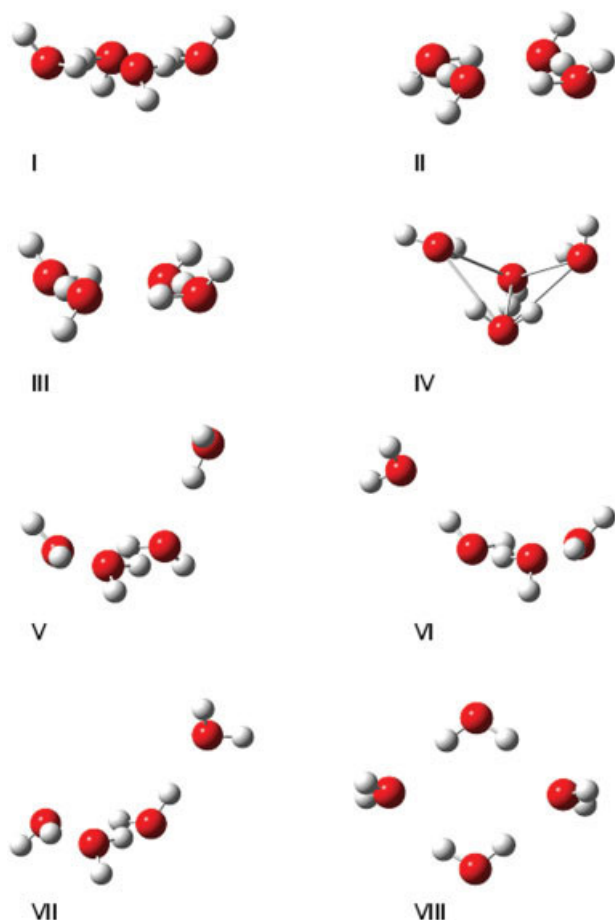
FIGURE 4. Geometrical motifs for the W_4 clusters at the B3LYP/6-311++G** and MP2/6-311++G** levels. O—O bonds are drawn on purpose on structure IV to help visualize the bicylce-like arrangement, however, those distances are of the order of 2.94 Å. To our knowledge, structures III and VII have not been previously reported. [Color figure can be viewed in the online issue, which is available at www.interscience.wiley.com.]

This energy ordering seems to suggest that cooperative polarization effects play an important role in the stabilization of small water clusters: the more stable structures (I, II, III) have four alternating dipole components (along the O—H bonds) on the same plane, the next one (IV) has four dipoles alternating off-plane, the next group (V, VI, VII) alternates three dipole moment components in the plane while the least stable (VIII) shows no cooperative polarization of the individual dipole moments. Table II also tells us that there are at least three isomers with significant populations, this result opposes the accepted view that only two isomers contribute to W_4 clusters.

An inventory of geometrical parameters and Mulliken charge distributions is shown in Table III. Like others before [8, 33], we observe shorter O—O atom distances when going from trimers (V, VI, VII) to tetramers (I, II, II); likewise, there seems to be a correlation between the charge difference in the atoms involved in the hydrogen bond networks (H_2 and O) and the relative stability of the clusters (Tables II and III); this observation suggest that

TABLE I _____

Literature information for the W_4 clusters obtained on the B3LYP/6-311++G and MP2/6-311 ++G** PESs.**

Structure	References	Method
I	[2]	MP2/6-311+G(2d,2p)
	[8]	PP (DFT)
	[10]	HF/6-31G*
	[28]	MP2 and ASP-W_n [29] potentials
	[30]	HF/DZP+, EFP, and ASP-W_n potentials
	[31]	MPW1PW91/aug-cc-pVDZ
	[32]	MP2 and ASP potentials
II	[30]	HF/DZP+, EFP, and ASP-W_n potentials
III		No previous reports
IV	[2]	MP2/6-311+G(2d,2p)
	[10]	HF/6-31G*
	[28]	MP2 and ASP-W_n potentials.
V	[10]	HF/6-31G*
VI	[10]	HF/6-31G*
VII		No previous reports
VIII	[2]	MP2/6-311+G(2d,2p)
	[10]	HF/6-31G*
	[28]	MP2 and ASP-W_n potentials.

Our methodology locates two structures not previously reported.

show the same energy ordering for the common isomers with very little difference in every other energetic aspect, i.e., very similar binding energies and isomer concentrations. The CCSD(T)//MP2 calculations do not make any appreciable difference in the calculated energies. The clusters are energetically ordered by their structural motifs: cyclic tetramers (all molecules are donor and acceptor) are more stable than the bicycle-like structure which in turn is more stable than tetramers containing cyclic trimers plus an additional water molecule, the least stable structure being the cyclic tetramer with doubly donor and doubly acceptor water molecules; within each group, energy differences are minimal.

TABLE II _____

Energetics and thermochemistry for W_4 clusters.

Quantity	I	II	III	IV	V	VI	VII	VIII
ΔE^a	0.00	1.05	1.14	6.72	7.91	7.91	7.77	13.41
ΔE^b	0.00	1.03	1.11	6.28	7.58	7.36	7.44	12.52
ΔE^c	0.00	1.03	1.10	5.89	7.30	7.09	7.17	12.02
BE^a	30.79	29.74	29.65	24.07	22.88	22.88	23.01	17.38
BE^b	31.32	30.28	30.21	25.04	23.73	23.96	23.87	18.79
BE^c	30.72	29.70	29.63	24.83	23.43	23.63	23.55	18.71
$\%x_i^a$	78	12	10	≈0	≈0	≈0	≈0	≈0
$\%x_i^b$	78	12	10	≈0	≈0	≈0	≈0	≈0
$\%x_i^c$	77	12	11	≈0	≈0	≈0	≈0	≈0
ZPE^b	63.23	62.98	63.05	62.24	62.04	62.07	61.93	60.92
$Gibbs^{b,d}$	42.35	41.59	41.59	40.36	38.68	39.22	38.54	37.28

Relative energies (ΔE), binding energies (BE), unscaled zero-point vibrational (ZPE), and Gibbs energies in Kcal/mol. Isomer populations ($\%x_i$) estimated with Eq. (1).
Quantities calculated at the following levels:
[a] B3LYP/6-311++G**.
[b] MP2/6-311++G**.
[c] CCSD(T)/6-311++G**//MP2/6-311++G**.
[d] Calculated as G = H − TS, T = 298.16 K.

cooperative charge transfer is also a determining factor in the stabilizing interactions of small water clusters. Geometrical and charge parameters seem to behave in analogous fashion to energy factors in the sense that clusters belonging to the same geometrical motifs do not exhibit large difference among them.

4. Conclusions and Perspectives

We have successfully applied the ASCEC methodology, which uses a modified Metropolis algorithm, to the exploration of the PES of the water tetramer. We found eight stationary points on the B3LYP/6-311++G** and MP2/6-311++G** surfaces (two unreported previously). The global minimum found by us is the same reported in previous works. The equilibrium geometries belong to three different geometrical motifs: four planar cyclic tetramers, three of them exhibiting the same hydrogen bonded network, where each water molecule acts simultaneously as hydrogen bond donor and acceptor; in the remaining tetramer, two opposing molecules act as double donors while the other two act as double acceptors of the hydrogen bonds;

TABLE III _____

Mulliken charges and geometrical parameters for W_4 clusters.

Structure	O—O	O—H_1	O—H_2	H_2—O	Q_{H_1}	Q_{H_2}	Q_O
I	2.74	0.96	0.98	1.77	+0.27	+0.36	−0.63
II	2.74	0.96	0.98	1.78	+0.27	+0.36	−0.63
III	2.75	0.96	0.98	1.79	+0.27	+0.37	−0.64
IV	2.94	0.96	0.98	2.0	+0.26	+0.30	−0.56
V	2.84	0.96	0.97	1.82	+0.28	+0.33	−0.61
VI	2.85	0.96	0.98	1.88	+0.26	+0.32	−0.58
VII	2.84	0.96	0.98	1.90	+0.27	+0.32	−0.59
VIII	3.00	0.96	0.97	2.04	+0.27	+0.31	−0.58

Atom distances in Angstroms. H_1 atoms do not belong to hydrogen bonds while H_2 atoms do. In cases where more than one possibility exists, an average was taken.

three planar cyclic trimers interacting with an extra off-plane water molecule and a bicycle-like conformation. The energy ordering follows the geometrical motifs in order of stability: (1) cyclic tetramers, (2) bicycle-like, (3) cyclic trimers + additional water, (4) cyclic tetramer, where molecules are doubly donor and doubly acceptor simultaneously. The stabilization of the water tetramers seems to come from two sources, cooperative polarization and cooperative charge transfer. Our calculations seem to suggest that at least three different isomers contribute significantly to the water tetramer.

References

1. Mejía, S.; Espinal, J.; Restrepo, A.; Modragón, F. J Phys Chem A 2007, 111, 8250.
2. Masella, M.; Gresh, N.; Flament, J. P. J Chem Soc 1998, 94, 2745.
3. Koch, W.; Holthausen, M. A Chemist's Guide to Density Functional Theory, 2nd ed.; Wiley: New York, 2002.
4. Chalasinski, G.; Szczesniak, M.; Cieplak, P.; Scheiner, S. J Chem Phys 1991, 94, 2873.
5. Ojamäe, L.; Hermannsson, K. J Phys Chem 1994, 98, 4271.
6. Masella, M.; Flament, J. J Chem Phys 1998, 108, 7141.
7. King, B.; Weinhold, F. J Chem Phys 1995, 103, 333.
8. Estrin, D.; Paglieri, L.; Corongiu, G.; Clementi, E. J Phys Chem 1996, 100, 8701.
9. Wales, D.; Walsh, T. J Chem Phys 1997, 17, 7193.
10. Miyake, T.; Aida, M. Int Electron J Mol Des 2003, 2, 24.
11. Restrepo, A.; Mari, F.; Gonzalez, C.; Marquez, M. Química, Actualidad y Futuro 1995, 5, 101.
12. Fletcher, R. Practical Methods of Optimization, Vol. 1; Wiley: New York, 1980.
13. Metropolis, N.; Rosenbluth, A.; Rosenbluth, M.; Teller, A.; Teller, E. J Chem Phys 1953, 21, 1087.
14. Kirkpatrick, S.; Gellat, C.; Vecchi, M. Science 1983, 220, 671.
15. Aarts, E.; Laarhoven, H. Simulated Annealing: Theory and Applications; D. Reidel Publishing: Dordrecht, The Netherlands, 1987.
16. Pérez, J.; Florez, E.; Hadad, C.; Fuentealba, P.; Restrepo, A. J Phys Chem A (in press).
17. Jhon, F. P.; Albeiro, R. ASCEC V-01: Annealing Simulado Con Energía Cuántica. Property, development and implementation: Grupo de Química-Física Teórica, Instituto de Química, Universidad de Antioquia, AA 1226 Medellín, Colombia.
18. Frisch, M. J.; Trucks, G. W.; Schlegel, H. B.; Scuseria, G. E.; Robb, M. A.; Cheeseman, J. R.; Montgomery, J. A., Jr.; Vreven, T.; Kudin, K. N.; Burant, J. C.; Millam, J. M.; Iyengar, S. S.; Tomasi, J.; Barone, V.; Mennucci, B.; Cossi, M.; Scalmani, G.; Rega, N.; Petersson, G. A.; Nakatsuji, H.; Hada, M.; Ehara, M.; Toyota, K.; Fukuda, R.; Hasegawa, J.; Ishida, M.; Nakajima, T.; Honda, Y.; Kitao, O.; Nakai, H.; Klene, M.; Li, X.; Knox, J. E.; Hratchian, H. P.; Cross, J. B.; Bakken, V.; Adamo, C.; Jaramillo, J.; Gomperts, R.; Stratmann, R. E.; Yazyev, O.; Austin, A. J.; Cammi, R.; Pomelli, C.; Ochterski, J. W.; Ayala, P. Y.; Morokuma, K.; Voth, G. A.; Sal- vador, P.; Dannenberg, J. J.; Zakrzewski, V. G.; Dapprich, S.; Daniels, A. D.; Strain, M. C.; Farkas, O.; Malick, D. K.; Rabuck, A. D.; Raghavachari, K.; Foresman, J. B.; Ortiz, J. V.; Cui, Q.; Baboul, A. G.; Clifford, S.; Cioslowski, J.; Stefanov, B. B.; Liu, G.; Liashenko, A.; Piskorz, P.; Komaromi, I.; Martin, R. L.; Fox, D. J.; Keith, T.; Al-Laham, M. A.; Peng, C. Y.; Nanayakkara, A.; Challacombe, M.; Gill, P. M. W.; Johnson, B.; Chen, W.; Wong, M. W.; Gonzalez, C.; Pople, J. A. Gaussian 03, Revision D. 01; Gaussian Inc.: Wallingford, CT, 2004.
19. Stewart, J. J Comput Chem 1989, 10, 209.
20. Stewart, J. J Comp Chem 1989, 10, 221.
21. Stephens, P.; Devlin, J.; Chabalowski, C.; Frisch, M. J Phys Chem 1994, 98, 11623.
22. Lee, C.; Yang, W.; Parr, R. Phys Rev B 1988, 37, 785.
23. Becke, A. J Chem Phys 1993, 98, 5648.
24. Moller, C.; Plesset, M. Phys Rev 1934, 46, 618.
25. Krishnan, R.; Pople, J. Int J Quant Chem 1978, 14, 91.
26. Pople, J.; Head-Gordon, M.; Raghavachari, K. J Chem Phys 1987, 87, 5968.
27. Albeiro Restrepo. Ph. D. Thesis, University of Connecticut, 2005.
28. Hodges, M.; Stone, A.; Xantheas, S. J Phys Chem A 1997, 101, 9163.
29. Millot, C.; Stone, A. Mol Phys 1992, 77, 439.
30. Merrill, G.; Gordon, M. J Phys Chem A 1998, 102, 2650.
31. Cabral, P.; Costa, B.; Canuto, S. Chem Phys Lett 2006, 429, 129.
32. Engkvist, O.; Åstrand, P.; Carlström, G. Chem Rev 2000, 100, 4087.
33. Cruzan, J.; Viant, M.; Brown, M.; Saykally, R. J. Phys. Chem. A. 1997, 101, 9022.